

# Realization of Color Constancy Using the Dichromatic Reflection Model

*Shoji Tominaga*

*Osaka Electro-Communication University, Neyagawa, Osaka, Japan*

## Abstract

A method is proposed for recovering both the surface-spectral reflectance function and the illuminant spectral-power distribution based on the dichromatic reflection model. A multi-band imaging device is realized by combining a monochrome CCD camera and several color filters, to separate the incident light into six wavelength bands throughout the visible spectrum. We show a measuring method to predict the spectral sensitivity functions of the imaging system. The dichromatic reflection for inhomogeneous objects is described using finite-dimensional models. The estimation algorithms are presented to recover the scene parameters in two steps from the image data. The illuminant spectrum of a projector lamp is recovered fairly well, and the Munsell color patches are estimated in the average accuracy of about  $\Delta E_{ab} = 3.5$ .

## Introduction

A number of algorithms are made to demonstrate computationally how color constancy may be accomplished. The computational color constancy has difficulty that estimation of both the illumination and reflectance is nonlinear, and it is an underdetermined problem due to many unknown parameters. A commonly used approach to reduce the number of parameters required to describe illuminants and surfaces have been to describe spectral functions using finite-dimensional linear models.<sup>2</sup> It is shown that the number of dimensions to describe measured daylights is approximately four. Moreover the number for measured surfaces in a natural scene lies somewhere between six and eight. Therefore it should be noted that linear models with dimension as low as three are insufficient for spectral description, although it captures a large percentage of the variance of the measured spectra. Nevertheless, so far, CCD color cameras of RGB outputs have been used as the imaging device, and moreover computer simulations using only synthetic images have been performed to evaluate the algorithms for color constancy.<sup>5,7</sup> A major difficulty in using a real camera is based on difficult prediction of the spectral sensitivity functions.

Most surfaces of both natural objects and artificial ones are composed of inhomogeneous materials like plastics. The surface spectral reflectance function of an inhomogeneous object is described as the sum of a constant interface (specular) reflectance and a body (diffuse) reflectance. This model for light reflection is called the dichromatic reflection model. The present paper describes a method for recovering both the surface-spectral reflectance function

and the illuminant spectral-power distribution based on the dichromatic reflection model. The interface component of the dichromatic reflection model is used for estimating the illuminant, while the body component determines an inherent reflection property of its surface. We realize a multi-band imaging device that consists of six wavelength bands throughout the visible spectrum by combining a monochrome CCD camera and several color filters. A measuring method is shown to predict accurately the spectral sensitivity function. The spectral power distribution of illuminant is estimated from a set of sensor outputs for inhomogeneous surfaces. The illuminant and the body reflectance function are described using finite dimensional models. Algorithms are presented to estimate the spectral shapes. It is shown that the illuminant spectrum and the body spectral reflectance functions are recovered fairly well on our multi-band imaging system.

## Imaging Device

The monochrome CCD camera used in this study is a Sony model XC-75 camera, and the lens is Nikon standard photographic lens of focal length 50 mm or 35 mm. First the linearity of the camera response was investigated using a calibrated CRT monitor. When uniform color patches were displayed successively on the monitor, the images and the emitted light intensities were measured, respectively, with the camera and a radiometer. Then we observed a linear relationship between the luminances of the incident light to the camera and the gray scale values of the camera output. The camera response is linear as  $\gamma = 1$ . Next the spectral characteristics for different parts of the imaging device were measured separately for predicting the whole spectral response of the system. Two kinds of optical filter are used here: a colored glass filter for suppressing infrared light, and some Kodak gelatin filters for selecting wavelength bands. The glass filter is inserted between the lens and the camera, and the gelatin filters are attached to the front of the lens.

The knowledge of the spectral-response function of the camera is crucial in estimating the illuminant and surface-spectral reflectance. Figure 1 shows the measuring system for the spectral sensitivity of the monochrome CCD camera without lenses. A set of 31 interference filters is used to convert the continuous spectrum of a projector lamp into a set of monochromes, which are in 31 equally spaced wavelength points throughout the visible region of 400-700 nm, as shown in Figure 2. Each monochromatic light is guided to diffusers, and the diffused transmission light is measured with both the camera and the radiometer. The spectral-

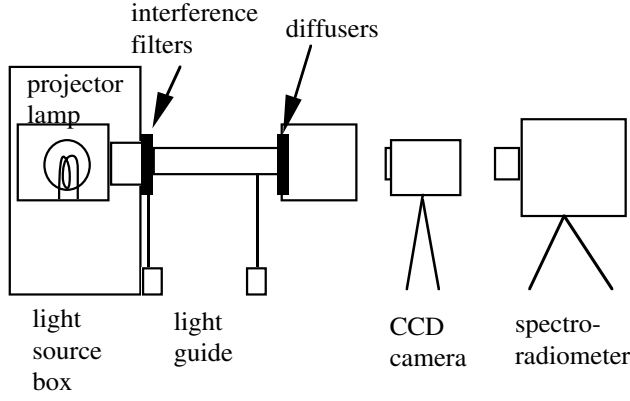


Figure 1. Measuring system for the spectral sensitivity of the camera

sensitivity function is then determined by taking the ratio of the camera output to the measured radiance at each wavelength point.

To build a multi-band imaging system with six color sensors, we combine Kodak Wratten filters in six wavelength bands of the visible region. The filters are selected so that the broad bands of the color components are little overlapped on the wavelength axis, and the transmitted lights have enough amount for imaging. The present filter combination for six color components is as follows: B: #47, BG: #44a + cc20g, G: #52, Y: #21 + cc50g + cc40g, R: #25 + cc20g + cc20g, R2: #29 + cc30g. The spectral sensitivity function of each sensor is calculated by multiplying the filters' transmittance and the original spectral sensitivity of the monochrome camera. Furthermore, to balance the six sensor quantum catches, we determined the weights for the sensor outputs by using a standard white reference. Figure 2 shows the whole spectral sensitivity functions of the sensors.

### Modeling for Dichromatic Reflection

The color signal  $C^o(x, \lambda)$  from an object number  $o$  is a function of the wavelength  $\lambda$ , ranging over a visible wavelength, and the location parameter  $x$ , including various geometric parameters under a fixed imaging geometry. The dichromatic reflection model suggests that light reflected from the surface of an inhomogeneous object is decomposed into two additive components, the body reflection and the interface reflection.<sup>3,8</sup> The color signal  $C^o(x, \lambda)$  is then expressed in the form

$$C^o(x, \lambda) = \alpha(x)S^o(\lambda)E(\lambda) + \beta(x)E(\lambda), \quad (1)$$

where  $S^o(\lambda)$  is the surface-spectral reflectance function of the object  $o$ , and  $E(\lambda)$  is the spectral power distribution of the illumination. The first term of the right-hand side in Eq. (1) represents the body reflection where  $\alpha(x)$  is its shading factor, while the second term represents the specular reflection where  $\beta(x)$  is the scale factor.

Suppose that the illumination  $E(\lambda)$  can be modeled by a linear finite-dimensional model

$$E(\lambda) = \sum_{i=1}^m \varepsilon_i E_i(\lambda) \quad (2)$$

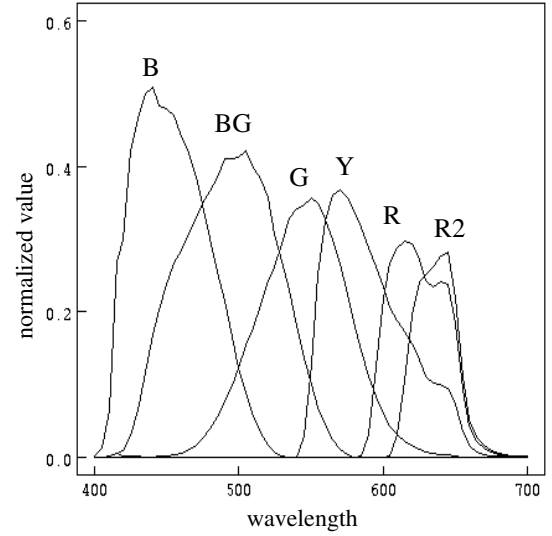


Figure 2. Spectral sensitivity functions of camera

with a statistically determined set of basis functions  $E_i(\lambda)$  ( $i = 1, 2, \dots, m$ ). Also suppose that the spectral reflectance function  $S^o(\lambda)$  can be represented in the same fashion with another basis  $S_j(\lambda)$  ( $j = 1, 2, \dots, n$ )

$$S^o(\lambda) = \sum_{j=1}^n \sigma_j^o S_j(\lambda). \quad (3)$$

We assume that there are 6 distinct classes of image sensors at each location  $x$ . The sensor responses  $\rho_k^o(x)$  from an object  $o$  are given in the form

$$\rho_k^o(x) = \int_{\lambda=400}^{700} C^o(x, \lambda) R_k(\lambda) d\lambda, \quad (4)$$

where  $R_k(\lambda)$  is the spectral sensitivity function for the  $k$ -th sensor.

Substituting the finite-dimensional model expression for  $E(\lambda)$  and  $S^o(\lambda)$  into (4) permits us to express the relationship between the sensor outputs and the scene parameters as

$$\bar{\rho}^o(x) = \alpha(x) \bar{\Lambda}_\varepsilon \bar{\sigma}^o + \beta(x) \mathbf{H} \bar{\varepsilon}, \quad (5)$$

where  $\bar{\rho}^o(x)$  is a column vector formed from 6 sensor responses  $\rho_k^o(x)$  ( $k = 1, 2, \dots, 6$ ). The matrix  $\bar{\Lambda}_\varepsilon$  is 6-by- $n$ , and its  $(k, j)$ -th entry is of the form

$$\sum_{i=1}^m \varepsilon_i \int S_j(\lambda) R_k(\lambda) d\lambda. \quad (6)$$

The matrix  $\mathbf{H}$  is 6-by- $m$ , and its  $(k, i)$ -th entry is of the form

$$\int E_i(\lambda) R_k(\lambda) d\lambda. \quad (7)$$

The vectors  $\bar{\sigma}^o$  and  $\bar{\varepsilon}$  are of dimensions  $n$  and  $m$ , respectively, which represent the weight vectors for surface reflectance and illuminant.

## Estimation Algorithms

From the image data for inhomogeneous objects in a scene, we would like to recover the unknown illumination spectrum  $E(\lambda)$  and the surface-spectral reflectance  $S^o(\lambda)$  for each object. That is, given the measured sensor values  $\bar{p}^o(x)$  for each surface, we estimate the illuminant vector  $\bar{\epsilon}$  and reflectance vector  $\bar{\sigma}^o$ . Here this estimation problem for two kinds of scene parameter is solved in two steps. First the illuminant vector is estimated from the observations of several object surfaces that include specular reflection. Next, by using the estimated illuminant vector, we recover the vector of a body reflectance function, unique to each surface, from the image data.

### Illuminant

The finite-dimensional model for dichromatic reflection in Eq. (5) indicates that the sensor output  $\bar{p}^o(x)$  at any spatial location  $x$  on the object surface  $\underline{o}$  is expressed as a linear combination of the two vectors  $\bar{\Lambda}_\epsilon \bar{\sigma}^o$  and  $\mathbf{H} \bar{\epsilon}$ . These two vectors represent two components of body reflection and interface reflection for camera data. Therefore the two vectors span a two-dimensional subspace (plane) in a six-dimensional vector space, and then all the sensor responses observed from the same object surface fall in this subspace. We may call this subspace the image-signal plane.

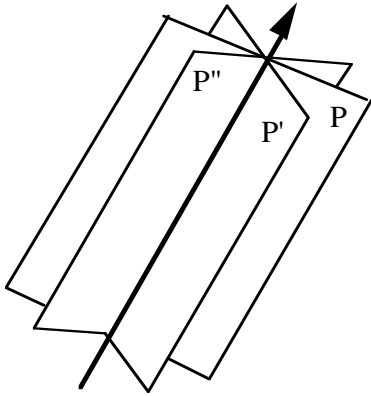


Figure 3. Intersection of image-signal planes.

Suppose that we observe  $M$  objects under the same illumination. The  $M$  image-signal planes must intersect because  $\mathbf{H} \bar{\epsilon}$  is contained in all planes, as shown in Figure 3. The matrix  $\mathbf{H}$  is calculated in advance from Eq. (7) with the illuminant basis functions and the camera spectral sensitivity functions. Therefore, if the intersection is found, the illuminant vector  $\bar{\epsilon}$  can be recovered from the intersection vector  $\mathbf{H} \bar{\epsilon}$  by a matrix inversion  $\mathbf{H}^{-1}$  or a pseudo-matrix inversion  $\mathbf{H}^+$ . In a previous paper<sup>3</sup>, Tominaga and Wandell presented an algorithm for finding the intersection of two planes in the case of two objects. In real scenes, there are not only smoothed surfaces with strong specular reflection like plastics, but also matte surfaces with only a little specularly like papers. A way to improve the illuminant estimation under the condition of weak specularly is to increase the number of object surfaces used in the estimation.

We propose a solution method for finding a reliable estimate of the common intersection vector for the general case of more than three objects. For simplicity of the

mathematical description, we assume  $M=3$  in the following. Let three pairs of vectors  $[\mathbf{u}_1, \mathbf{u}_2]$ ,  $[\mathbf{u}'_1, \mathbf{u}'_2]$ , and  $[\mathbf{u}''_1, \mathbf{u}''_2]$  be the orthonormal bases that define the image-signal planes  $P$ ,  $P'$ , and  $P''$ , respectively. The basis vectors are determined from the SVD of the six-dimensional camera data for the corresponding surface. If the planes  $P$ ,  $P'$ , and  $P''$  are intersect at a common line, the intersection line must lie in all the three planes. So we have three relations

$$\begin{aligned} c_1 \mathbf{u}_1 + c_2 \mathbf{u}_2 &= c'_1 \mathbf{u}'_1 + c'_2 \mathbf{u}'_2 \\ c'_1 \mathbf{u}_1 + c'_2 \mathbf{u}_2 &= c''_1 \mathbf{u}_1 + c''_2 \mathbf{u}_2 \\ c_1 \mathbf{u}_1 + c_2 \mathbf{u}_2 &= c_1 \mathbf{u}_1 + c_2 \mathbf{u}_2 \end{aligned} \quad (8)$$

These relations are equivalent to the homogeneous equation

$$\begin{bmatrix} \mathbf{u}_1 & \mathbf{u}_2 & -\mathbf{u}'_1 & -\mathbf{u}'_2 & 0 & 0 \\ 0 & 0 & \mathbf{u}'_1 & \mathbf{u}'_2 & -\mathbf{u}''_1 & -\mathbf{u}''_2 \\ \mathbf{u}_1 & \mathbf{u}_2 & 0 & 0 & -\mathbf{u}''_1 & -\mathbf{u}''_2 \end{bmatrix} \begin{bmatrix} c_1 \\ c_2 \\ c'_1 \\ c'_2 \\ c''_1 \\ c''_2 \end{bmatrix} = 0. \quad (9)$$

A nontrivial solution of the above equation defines the intersection line. A numerical solution might be obtained by applying the SVD algorithm to the  $18 \times 6$  coefficient matrix in Eq. (9).

### Reflectance

Once the illuminant vector is known, we solve for surface reflectances. If the observed surfaces to be recovered include no such interface reflection component as specular highlight, the reflectance estimation is straightforward. The lighting matrix  $\bar{\Lambda}_\epsilon$ , depending on the illuminant vector, is explicitly computed from Eq. (6). The surface reflectance vector can then be computed in the form

$$\bar{\sigma}^o = \bar{\Lambda}_\epsilon^+ \bar{p}^o(x), \quad (10)$$

where  $\bar{\Lambda}_\epsilon^+$  is the  $n$ -by-6 pseudoinverse of  $\bar{\Lambda}_\epsilon$ . Since the vector  $\bar{\sigma}^o$  in Eq.(10) still contains the influence of the shading factor, the normalized vector is obtained as the estimate.

If the observed surfaces include any specular reflection, and so possess the dichromatic reflection property, then we determine a unique estimate of the body reflection function for each surface from the observations on the image-signal plane. Because of two dimensionality on the image-signal plane, the body reflection vector  $\bar{\Lambda}_\epsilon \bar{\sigma}^o$  can be represented in terms of two orthonormal vectors  $[\mathbf{H} \bar{\epsilon}]$  and  $[\mathbf{H} \bar{\epsilon}]^\perp$  as

$$\bar{\Lambda}_\epsilon \bar{\sigma}^o = c_\epsilon [\mathbf{H} \bar{\epsilon}] + c_\epsilon^\perp [\mathbf{H} \bar{\epsilon}]^\perp, \quad (11)$$

where  $[\mathbf{H} \bar{\epsilon}]^\perp$  is a unit length vector perpendicular to  $[\mathbf{H} \bar{\epsilon}]$  on the plane. A permissible solution band for the coefficients  $(c_\epsilon, c_\epsilon^\perp)$  is given by applying an extended quarter-circle analysis<sup>4</sup>. A reliable estimate of the vector  $\bar{\Lambda}_\epsilon \bar{\sigma}^o$  is obtained as the data point on the plane that is farthest away from the illuminant vector  $[\mathbf{H} \bar{\epsilon}]$ . The reflectance vector  $\bar{\sigma}^o$  is finally recovered in the same way as in Eq.(10).

## Experiments

To determine a set of the illuminant basis functions, we analyzed nine spectra from representative light sources that were the daylight spectra of D55, D65, and D75, the CIE standard light spectra of A, B, and C, and the measured spectra of real sunlight, a slide projector, and a tungsten halogen lamp. The first three principal-component vectors for this set of spectra are used as  $E_i(\lambda)$  ( $i = 1, 2, 3$ ). In an experiment of illuminant estimation we measured three sheets of colored papers that were wrapped around a cylinder under the illumination of a slide projector. Weak specular highlights appeared on the object surfaces. Figure 4 shows the illuminant estimation result from the algorithm for finding an intersection of three image-signal planes. One curve represents the estimated illuminant from the camera data, and another is the direct measurement with a spectroradiometer.

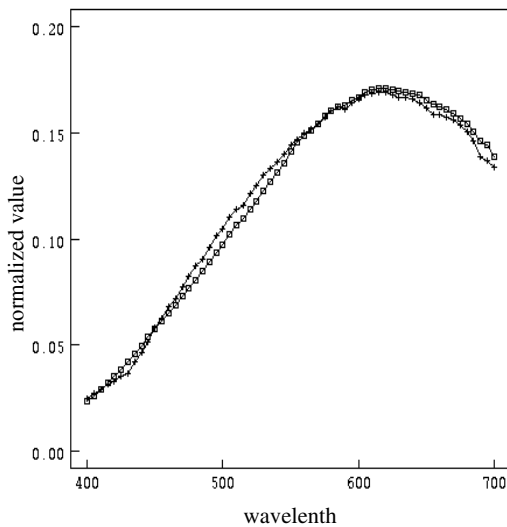


Figure 4. Estimation results of illumination

Next, the database of surface-spectral reflectances provided by Eastman Kodak Company was analyzed for the reflectance basis functions. This database consists of 354 measured spectral reflectances from various objects. We use the first five principal-component vectors as the basis reflectances  $S_j(\lambda)$  ( $j = 1, 2, \dots, 5$ ). The reflectance estimation was done based on the above algorithms using these reflectance basis functions and the estimated illuminant. The accuracy of the reflectance estimation was examined using the Macbeth Color Checker. The CIE  $L^*a^*b^*$  color difference was used as the measure of estimation error. The average error was  $\Delta E_{ab} = 3.53$  under the above illumination and basis functions. This error includes both errors on illuminant and reflectance.

Furthermore the surfaces of three plastic objects, including strong specular highlights, were measured under the illumination a halogen lamp. By the same procedure, the illuminant and the spectral reflectances were recovered from the camera data.

## Conclusion

This paper has proposed a method for recovering both the surface-spectral reflectance function and the illuminant spectral-power distribution based on the dichromatic reflection model. A multi-band imaging device is realized by combining a monochrome CCD camera and several color filters. This system separates the incident light into six wavelength bands throughout the visible spectrum, and get the corresponding color component images to the six bands. We show a measuring method to predict the spectral sensitivity functions of the imaging system. The dichromatic reflection for inhomogeneous object surfaces is described in finite-dimensional models. The estimation algorithms are presented to recover the scene parameters of the illuminant and the surface reflectances in two steps from the image data. The experimental results show that a suitable finite-dimensional model is given with three basis functions for the illuminant and five basis functions for the reflectances. The illuminant spectrum of a projector lamp is recovered fairly well, and the Macbeth color patches are estimated in the average accuracy of about  $\Delta E_{ab} = 3.5$ .

## References

1. G. Buchsbaum, A spatial processor model for object colour perception, *J. of the Franklin Institute*, **310**, 1-26, 1980.
2. L. T. Maloney and B. A. Wandell, A method for recovering surface spectral reflectance, *J. Opt. Soc. Am. A*, **3**, 29-33, 1986.
3. S. Tominaga and B. A. Wandell, The standard surface reflectance model and illuminant estimation, *J. Opt. Soc. Am. A*, **6**, 576-584, 1989.
4. S. Tominaga, Surface identification using the dichromatic reflection model, *IEEE Trans. PAMI*, **13**, 658-670, 1991.
5. M. S. Drew, Optimization approach to dichromatic images, *J. Math. Imaging and Vision*, **3**, 187-203, 1993.
6. B. V. Funt, Modelling reflectance by logarithmic basis functions, *1st Color Imaging Conf.*, 1993; (see page 291, this publication).
7. D. H. Brainard and W. T. Freeman, Bayesian method for recovering surface and illuminant properties from photosensor responses, *IS&T/SPIE Symposium*, 1994; (see page 344, this publication).
8. S. A. Shafer, Using color to separate reflection components, *Color Res. and Appl.*, **10**, 210-218, 1985.

published previously in the IS&T 1994 Color Imaging Conference Proceedings, page 37